Effects of Branch Points and Chain Ends on the Thermodynamic Interaction Parameter in Binary Blends of Regularly Branched and Linear Polymers

ARTICLE *in* MACROMOLECULES · JUNE 2006

Impact Factor: 5.8 · DOI: 10.1021/ma060023j

2 AUTHORS, INCLUDING:

Mark D. Foster
University of Akron
195 PUBLICATIONS **2,483** CITATIONS

SEE PROFILE

Effects of Branch Points and Chain Ends on the Thermodynamic Interaction Parameter in Binary Blends of Regularly Branched and Linear Polymers

Jae S. Lee and Mark D. Foster*

Maurice Morton Institute of Polymer Science, The University of Akron, Akron, Ohio 44325

David T. Wu

Chemical Engineering Department and Chemistry Department, Colorado School of Mines, Golden, Colorado 80401

Received January 4, 2006; Revised Manuscript Received May 15, 2006

ABSTRACT: The architectural effects of branch points and chain ends on the bulk thermodynamic interaction parameter, χ_{eff}, in binary blends of branched polymers with their linear analogues have been investigated using small-angle neutron scattering (SANS) and a series of well-defined, regularly branched polystyrenes with the same molecular weight and differing only in the number of branch points or chain ends. The value of χ_{eff} increases as the number of branch points increases for constant number of chain ends or as the number of chain ends increases for constant number of branch points. A Gaussian field theory for an athermal blend predicts the general trend in bulk χ_{eff} with the number of chain ends but does not capture the changes in χ_{eff} with changes in the number of branch points. Differences in chemistry among the various branch points probably have to be included to quantitatively predict changes in χ_{eff} for shorter branches. Qualitative variations in the size of the branched molecules in solution compare favorably with a Gaussian model for the branched chain's radius of gyration. The variation in the average statistical segment length with chain architecture was also determined from the SANS data.

Introduction

Polymer blending is one of the most versatile methods for modifying the properties of materials. Blends containing branched polymers are of particular interest[1−5] as they present possibilities for tailoring both bulk and surface physical properties[6] without large changes in the chemical nature of the material. Tailoring both bulk and surface properties of blends requires a knowledge of the bulk thermodynamics. For linear binary blend systems it is well-known that the bulk thermodynamics varies with molecular weight differences,[7] chemical microstructure,[8,9] tacticity,[10,11] and isotopic labeling[12,13] of the components. However, experimental studies on the effects of long-chain branching have been undertaken only by a few groups.

In an early study, Faust et al.[14] found when changing the architecture from linear to 22-arm star of the PS ((1.26−1.28) $\times$ 10^6 g/mol) component in a blend with poly(vinyl methyl ether) [PVME] (0.99 $\times$ 10^5 g/mol) the minimum temperature in the LCST did not shift, but the shape of the LCST curve changed subtly. On the other hand, Russell et al.[15] reported a shift up in the cloud-point curve of 10 °C when the architecture of a PS chain was changed from that of a linear to a 4-arm star in a blend of PS and poly(vinyl methyl ether). The discrepancy between the results from the two groups was likely due to the magnitude of the observed changes with architecture being smaller than the experimental uncertainties in determining the cloud-point temperature. Recently, Chen et al.[16,17] studied the effect of long-chain branching on the miscibility of blends of poly(ethylene-*r*-ethylethylene) (PEE). One of the random copolymer components had only short-chain (ethylethylene) branching, while the other had comb-type random branching as well as the short-chain branching. The long-chain branching was found to significantly narrow the miscibility window for these polyolefin blends.

Greenberg et al.[18−20] experimentally measured for the first time the effect of regular, long-chain branching on the thermodynamic interaction parameter in blends using well-defined 4-, 5-, and 6-arm star PS molecules in isotopically labeled blends with linear chains. From SANS data Greenberg et al. estimated the value of χ_ϵ, the entropic contribution to the interaction parameter due to long-chain branching alone, by assuming that χ_{eff} could be represented by a sum of χ_ϵ and $\chi_{isotopic}$, where $\chi_{isotopic}$ describes the interaction due to the isotopic difference. They also assumed that the value of $\chi_{isotopic}$ could be measured experimentally using a linear/linear isotopic blend in which the chain lengths of the component matched those of the star/linear blend. The magnitude of χ_ϵ was found to increase with the number of arms of the star and decrease with increasing length of the arms in qualitative agreement with the theory of Fredrickson et al.,[21] which we review below. While reasonable agreement between theory and experiment is found for blends with stars having fewer than 10 arms, the experimental values of χ_ϵ are substantially below the theoretical values for cases of stars having more than 10 arms, as shown in the Appendix. Martter et al.[22] measured the value of χ_{eff} for blends of linear and well-defined star polybutadienes with SANS. The magnitude of χ_ϵ varied in a nonmonotonic fashion: χ_ϵ(12-arm) > χ_ϵ(4-arm) > χ_ϵ(6-arm) > χ_ϵ(8-arm). However, qualitative agreement with the theoretical predictions from Fredrickson's group[21] was found in two aspects: χ_ϵ decreased with increasing concentration of the star, and χ_ϵ decreased with increasing size of the star arms. A measurement of the interaction[23] in star/linear blends of PMMA synthesized by atom transfer radical polymerization (ATRP) found that the value of χ_ϵ increased

* Corresponding author: Tel 330-972-5323; Fax 330-972-5290; e-mail mfoster@uakron.edu.

10.1021/ma060023j CCC: $33.50
Published on Web 07/01/2006

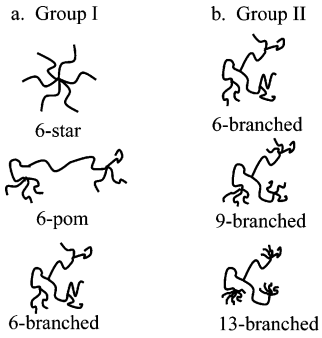

Figure 1. Structures and abbreviated names for the highly branched polystyrenes in group I, for which the number of end groups is fixed at 6 and the number of branching points varies from 1 to 4, and in group II, for which the number of end groups varies from 6 to 13 and the number of branching points is fixed at 4.

monotonically with the number of arms up to 14. Hutchings et al.[24] investigated melts of 3-, 4-, 8-, and 12-arm stars with one deuterium-labeled arm. They reported that the stretching of the arms increased with the number of arms. The R_g of the deuterated arm of the 8-arm star with an arm molecular weight of 33K was 8% larger than the value expected from the Gaussian approximation, and for the 12-arm star with 31K arms the stretching increased to 30%. However, they did not observe a clear trend in the variation of χ_{eff} with the number of arms. In this work, we have extended the study of the effect on bulk thermodynamics to more general chain architectures. In the prior studies with stars, the number of arms was always equal to the number of chain ends, and the star center was the only branch point. Here, we have separated the effects of chain ends and branch points in the chain architecture by studying two groups of novel, well-defined, highly branched polystyrenes prepared by anionic polymerization.[25] In one group the number of branch points in the molecule was varied from 1 to 2 to 4, and the number of ends was fixed at 6. In a second group the number of branch points in each molecule was fixed at 4, and the number of ends varied among 6, 9, and 13 as shown in Figure 1.

Field Theory for Architectural Contributions to χ

We briefly review the general approach of Fredrickson et al.[21] for calculating the free energy of mixing for binary blends of polymers due to differences in either short-chain or long-chain branching architecture, which we then apply below to the branched polymers studied in this paper. In this coarse-grained approach, the chains are assumed to be long enough for their conformations to be described by Gaussian statistics, with statistical segments of type i chains having length a_i and volume v_i. An excess contribution to the free energy occurs because the conformational fluctuations of a given polymer chain, and hence its entropy, are affected by the density fluctuations of the surrounding chains. The length scale and magnitude of these density fluctuations differ for chains of different architecture. By capturing the effects of these density fluctuations to Gaussian order, the total free energy density of mixing, ΔF, can be written

$$\frac{\Delta F}{k_B T} = \frac{\phi_1}{V_1}\ln\phi_1 + \frac{\phi_2}{V_2}\ln\phi_2 + \frac{F^E}{k_B T} \tag{1}$$

where the excess free energy density (neglecting terms linear in ϕ_1 and ϕ_2)

$$\frac{F^E}{k_B T} = \frac{1}{2(2\pi)^3}\int \ln[\phi_1 S_1(q) + \phi_2 S_2(q)]\, d\mathbf{q} \tag{2}$$

is given as an integral involving the pure-component single polymer structure factors $S_i(q)$. In the above, V_i is the total volume of a chain of type i, and ϕ_i is the volume fraction of that chain in the blend.

Within Flory−Huggins theory, the excess free energy density is assumed to be of the quadratic form $\alpha\phi_1(1-\phi_1)$, and the traditional Flory interaction parameter is then given simply as

$$\chi = \alpha(\nu_1\nu_2)^{1/2} \tag{3}$$

where we have assumed incompressibility of the polymer, i.e., $\phi_2 = 1 - \phi_1$. An architectural contribution to the interaction energy density, α, can then be associated with an appropriately normalized second derivative of F^E with respect to $\phi \equiv \phi_1$:

$$\alpha_\epsilon \equiv -\frac{1}{2k_B T}\frac{\partial^2 F^E}{\partial\phi^2} = \frac{1}{8\pi^2}\int_0^{\Lambda_b} q^2\left[\frac{S_1(q) - S_2(q)}{\phi S_1(q) + (1-\phi)S_2(q)}\right]^2 dq \tag{4}$$

The subscript ϵ denotes the entropic origin of this contribution to the interaction energy density. A high wavevector cutoff, $\Lambda_b \sim (a_1 a_2)^{-1/2}$, is introduced to control a divergence of the integral that occurs at that length scale for the "conformationally asymmetric" case of differing statistical segment lengths, $a_1 \neq a_2$. As discussed below, since the polymers studied here differ only in their long-branch architecture, we assume the statistical segment lengths of different chains are essentially equal (at least locally) and can perform the integral for α_ϵ above without a cutoff (i.e., $\Lambda_b \to \infty$).

Fredrickson et al. applied this approach to blends of branched and linear chains in which the repeat unit chemistries of the two chains were identical and the branched polymer was a star-branched or a regular comb-branched chain.[21] They calculated corrections to the Flory−Huggins theory to account for the entropic effect of the long-chain branching, assuming that the long chain branch obeyed Gaussian statistics with the same statistical segment length as the linear chain. Consequently, within a Gaussian model for conformations, the architectural contribution to χ arises from differences in the single-chain structure factors at length scales corresponding to the branching features on the branched polymer (arm lengths, distance between branch joints, etc.) and thus depends only on parameters describing the coarse-grained architecture.

For blends of star and linear homopolymers, the entropic contribution to the interaction free energy density, α_ϵ, is expressed in terms of the number of arms, p, and the arm radius of gyration, $R_2 = \sqrt{N_2 a^2/6}$, of the star polymer, where N_2 is the number of segments in an arm. For star polymers with a large number of short arms or for large homopolymers for which the condition of $(p-3)(R_1/R_2)^2 \gg 1$ is met, with R_1 being the radius of gyration of the linear chain, the approximate *universal* form of α_ϵ is given as

$$\alpha_\epsilon \approx \frac{1}{64\pi\sqrt{2}}\frac{(p-3)^{3/2}}{(1-\phi_1)^{1/2}R_2^3} \tag{5}$$

where ϕ_1 is the volume fraction of the linear component and is not too close to unity. This universal expression suggests that χ_ϵ, the entropic contribution to χ, should increase with the number of arms in the star, decrease with an increase in the length of the arm, and decrease with an increase in the concentration of the star. Note that this is consistent with the picture that high-functional branch points with short arms have a much greater density−density correlation function on short

Table 1. Molecular Characterization of the Branched Polystyrenes and Linear Analogues

polymer	name	arm M_n[a] (g/mol)	precursor M_n[a] (g/mol)	total M_n[a] (g/mol)	N[b]	M_w/M_n	α[c]	ω[d]
linear	linear			40 000	381	1.02	0	2
6-arm star	6-star	6300		36 300	345	1.04	1	5.8
6-end pom-pom	6-pom	3800	18 200	40 500	386	1.03	2	5.8
6-end branch	6-branch	3000	18 100	35 800	341	1.02	4	5.9
9-end branch	9-branch	2400	17 700	38 900	370	1.02	4	9.0
13-end branch	13-branch	1300	17 700	34 200	322	1.04	4	13.0
deuterated linear	*d*-PS			36 000	316	1.02	0	2

[a] Determined by GPC with three detectors: refractometer, viscometer, and light scattering. [b] Number of segments determined with a segment volume of 100 cm^3/mol. [c] Number of branch points. [d] Number of chain ends.

length scales in comparison with a linear chain. The size of the linear chain plays no role in the universal expression.

Theoretical studies on blends of a linear and a branched polymer having long chain branches have also been carried out by other research groups.[26−30] The Schweizer group used the polymer reference interaction site model (PRISM) theory to investigate the influence of chain branching on bulk thermodynamics.[26−28] Their calculations of χ_ϵ in star/linear blends[27,30] suggested a weaker dependence of χ_ϵ on the number of arms than predicted by the field theory. They suggested that for sufficiently long linear chains the dependence of χ_ϵ on the number of arms nearly disappeared or reversed.

None of the theories have specifically considered the pom-pom or end-branched structures studied here. In this paper, we will apply the Gaussian field theory described above, using single-chain structure factors corresponding to the given polymer branching architecture, assuming Gaussian conformations. The parameters entering the structure factors, such as the statistical segment length and arm molecular weights, will be those extracted from experimental data. This will allow a direct prediction for the entropic contribution to χ due solely to long-chain architectural differences. The comparisons with the measurements will also suggest some aspects of the experimental systems that remain to be captured theoretically.

Experimental Section

Materials. Linear hydrogenous and deuterated polystyrenes were synthesized anionically in benzene with *sec*-BuLi initiator. The living arm poly(styryl)lithium for the 6-arm star polymer was also prepared with *sec*-BuLi, and it was then end-capped with one or two units of butadiene to reduce the steric hindrance during the linking reaction while minimizing the effect of the presence of the butadiene units on bulk thermodynamics. All living arm polymers linked at a junction point to form the 6-end pom-pom polystyrene, 6-end branched PS, 9-end branched PS, or 13-end branched PS were also end-capped using one or two units of butadiene. The exact amount of butadiene attached to each arm polymer was determined using ^{1}H NMR and MALDI−TOF mass spectrometry. The molecular weights of the arm polymers were varied from 6000 to 1200 g/mol, depending on the number of end groups in the molecule, to achieve the same overall molecular weight. The living arm polymer for the 6-arm star polymer was coupled with 1,2-bis-(dichloromethylsilyl)ethane. The precursor polystyrene for the 6-end pom-pom PS was initiated with a difunctional initiator and polymerized anionically in benzene. The two living end groups were end-capped with excess tetrachlorosilane. Finally, the excess living arm polymer was coupled with the chlorosilyl end-functionalized precursor polymer. The precursor polymers for the 6-end branched, 9-end branched, and 13-end branched polystyrenes were prepared using a trifunctional initiator. The three chain ends of the precursor polymer were end-capped with excess methyltrichlorosilane, tetrachlorosilane, or 1,2-bis(trichlorosilyl)ethane to create the 6-end, 9-end, and 13-end branched polymers, respectively. The two precursor polymers for the 6-end and 9-end branched polymers were reacted directly with an excess of the appropriate living arm polymer. However, the 13-end branched polymer was prepared using a recently developed methoxysilyl functionalization method.[31] All chlorides of the chlorosilyl end-functionalized precursor polymer were converted into methoxy groups in order to be able to remove the excess linking agent by precipitation. Then the methoxysilyl end-functionalized precursor polymer was reacted with excess living arm polymer. All of the reaction product mixtures containing the final branched polymers were fractionated to eliminate uncoupled arms. The synthesis conditions and properties for each branched polymers are described in detail elsewhere.[25] The number of arms in each branched polymer was determined by characterizing the arm polymer, the precursor polymer, and then the branched polymer by gel permeation chromatography with three types of inline detection: refractive index measurement, differential pressure measurement, and light scattering. The number of end groups (f) was calculated from the molecular weights of the arm polymers, precursor polymer, and branched polymer, except for the 6-arm star polymer and the linear polymer, using the following equation:

$$f = \frac{M_{n,branched} - M_{n,precursor}}{M_{n,arm}} \quad (6)$$

Table 2. Butadiene Composition and Solution Properties of the Branched Polystyrenes and Linear Analogues

polymer	total BD wt % in branched PS[a]	$[\eta]$[b] (cm^3/g)	g'[c]	R_h (Å)[d]
linear		20.2	/	46.7
6-star	1.1	10.2	0.51	36.5
6-pom	1.5	17.5	0.87	43.3
6-branch	1.4	12.8	0.64	40.5
9-branch	1.8	11.7	0.58	36.8
13-branch	2.6	9.6	0.47	36.2

[a] Calculated using BD (wt %) = 100 × [54 × BD unit/M_n of branched PS] (±5%) from the data determined by ^{1}H NMR and MALDI-TOF. [b] Determined in toluene at 35 °C (±0.005). [c] Branching factor; $g' = [\eta]_{star}/[\eta]_{linear}$ (±0.04). [d] Determined by dynamic light scattering in toluene at 25 °C (±2.0 Å).

The molecular weights of all the branched polymers and linear analogues were controlled to be ∼36 000 g/mol to exclude effects on the interaction parameter due to molecular weight differences between the two components in a blend. The molecular characterizations of the chain functionalities and the molecular weights for each branched polymer and a linear analogue are summarized in Table 1. Molecular properties for the polymers reported in ref 25 are reproduced in Table 2 for convenience. The values of branching factor, g', which were calculated using intrinsic viscosity data measured at 35 °C in toluene, were in good agreement with calculations made using an expression for irregularly branched chains from Zimm and Stockmayer.[32] They were also consistent with hydrodynamic radii of the polymers measured in good solvent (toluene) with dynamic light scattering at 25 °C.

Sample Preparation. Blends containing 50 vol % branched hydrogenous polymers with the deuterated linear analogue were prepared by dissolution of the polymer in toluene. Solutions were filtered five times with 0.2 μm pore Whatman anotop 25 (Whatman International Ltd.) filters and then directly cast into films in Teflon beakers, allowing 3 days in a fume hood for evaporation of the solvent. The films were then dried under roughing vacuum at 70 °C for 7 days to ensure removal of the excess toluene. The dried

polymer blend films were pressed inside 1 mm thick brass washers having an inner diameter of 1 cm. To obtain transparent, bubble-free films, the samples were pressed at 120 °C under 3000 kg between pieces of Mylar foil.

Measurements. SANS measurements were performed on the NG3 30-m SANS instrument at the Cold Neutron Research Facility of the National Institute for Standards and Technology (Gaithersburg, MD). A neutron beam with a nominal wavelength of 6 Å and a spread ($\Delta\lambda/\lambda$) of 0.15 full width at half-maximum was used. Measurements were taken at a sample-to-detector distance of 4.5 m, providing a range of values of the scattering vector q of 0.007−0.14 Å^{-1}. The samples, sandwiched between quartz windows, were placed in sample holders provided by the National Institute of Standards and Technology laboratory. The sample holders were then placed inside a seven-slot computer-controlled aluminum sample changer, the temperature of which could be controlled between room temperature and 225 °C (±0.1 °C). Sample temperatures were varied from 120 to 200 °C in steps of 20 °C. This sample changer sat inside a stainless steal vacuum chamber that was evacuated to 450 μmHg and then backfilled with nitrogen gas to obtain a slight positive pressure, and this positive pressure was maintained throughout the measurement. Equilibration times of about 15 min were allowed after each set-point change. In addition to measurements of the samples, data were collected with the beam blocked, for an empty quartz-windowed cell, and with the instrument empty for estimating the background and empty cell contributions. Exact sample thickness was measured to normalize the raw data. To correct for incoherent scattering, 100% hydrogenous PS and 100% deuterated linear analogue samples were measured.

Results and Discussion

SANS Fitting and Single-Chain Structure Factors. The absolute coherent scattering intensity, $I(q)$, obtained from a binary isotopic blend of monodisperse polymers is related to the structure factor $S(q)$ of the blend by

$$I(q) = \frac{(b_1 - b_2)^2}{V} S(q) \tag{7}$$

where V is a reference volume, b_i is the coherent scattering length for polymer i averaged over the reference volume, and q is the scattering vector. The structure factor for a binary blend of polymers is given in the random phase approximation (RPA) for an incompressible, isotopic melt as[33]

$$S^{-1}(q) = \frac{1}{N_1\phi_1 S_1(q)} + \frac{1}{N_2\phi_2 S_2(q)} - 2\chi_{\text{eff}} \tag{8}$$

where ϕ_i is the volume fraction of component i, N_i is the number of segments in the chains of polymer i, and χ_{eff} is the effective thermodynamic exchange interaction parameter on a per segment basis. $S_1(q)$ and $S_2(q)$ are the form factors which capture the characteristics of the single polymer chains 1 and 2. The form factor for each polymer architecture was obtained through manipulation of the expressions given by Benoit[34] and Hammouda.[35]

The form factor for linear polymers within the Gaussian chain approximation is the well-known Debye function, $D(x)$:

$$S_{\text{lin}}(q) = D(x) = \frac{2(e^{-x} - 1 + x)}{x^2} \tag{9}$$

where $x = q^2R_g^2$ and $R_g^2 = N_{\text{lin}}a^2/6$ is the squared radius of gyration of the linear polymer. N_{lin} is the number of segments in the linear polymer, and a is the statistical segment length.

The form factor of a star polymer can be obtained by considering the correlations between the segments when the arms are identical. There are two types of correlations. One is the correlation between two segments in the same arm, which is described by the correlation function $S_{\text{BB1}}(q)$. The other is the correlation between segments in two different arms and is described by the correlation function $S_{\text{BB2}}(q)$. The expressions of $S_{\text{BB1}}(q)$ and $S_{\text{BB2}}(q)$ are given by

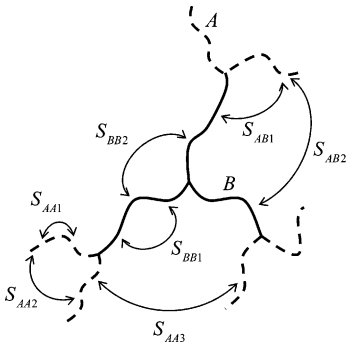

Figure 2. Structure of a 6-end branched polymer showing the possible interactions between various segments.

$$S_{\text{BB1}}(q) = D(x') = \frac{2(e^{-x'} - 1 + x')}{x'^2} \tag{10}$$

$$S_{\text{BB2}}(q) = F(x')^2 = \left(\frac{1 - e^{-x'}}{x'}\right)^2 \tag{11}$$

where $F(x')$ denotes the correlation function between two arms, $x' = q^2R_{\text{g,arm}}^2$, and $R_{\text{g,arm}}^2 = n_Ba^2/6$ is the squared radius of gyration of the branch. n_B is the number of segments in the branch. The form factor of a star polymer can be expressed by considering all possible correlations among the segments and number of arms, f:

$$S_{\text{star}}(q) = \frac{1}{f} S_{\text{BB1}}(q) + \frac{f-1}{f} S_{\text{BB2}}(q) \tag{12}$$

The form factors for the 6-end pom-pom, 6-end branch, 9-end branch, and 13-end branch chains can be obtained similarly. As an example, the correlations contributing to the form factor for the 6-end branched polymer are depicted in Figure 2. The form factor can be expressed as the sum of three major contributions:

$$S_{\text{branch}}(q) = \frac{N_B^2}{N^2} S_{\text{BB}}(q) + \frac{N_A^2}{N^2} S_{\text{AA}}(q) + 2\frac{N_AN_B}{N^2} S_{\text{AB}}(q) \tag{13}$$

where N is the total number of segments of the molecule ($N_A + N_B$), N_B is the total number of segments of the inside chains ($N_B = f_Bn_B$), and N_A is the total number of segments of outside branches ($N_A = f_An_A$). n_A and n_B are the number of segments in each outer branch and each inside branch, respectively, and f_A and f_B are the number of outside branches and inside branches, respectively. In eq 13, $S_{\text{BB}}(q)$ describes the correlation between segments in a branch of the precursor polymer (B) and is given by

$$S_{\text{BB}}(q) = \frac{1}{f_B} S_{\text{BB1}}(q) + \frac{f_B - 1}{f_B} S_{\text{BB2}}(q) \tag{14}$$

$$S_{\text{BB1}}(q) = D(x_B), \qquad S_{\text{BB2}}(q) = F(x_B)^2 \tag{15}$$

where $x_B = q^2n_Ba^2/6$. The correlation function $S_{\text{BB}}(q)$ for the precursor is that for a star polymer. The function describing

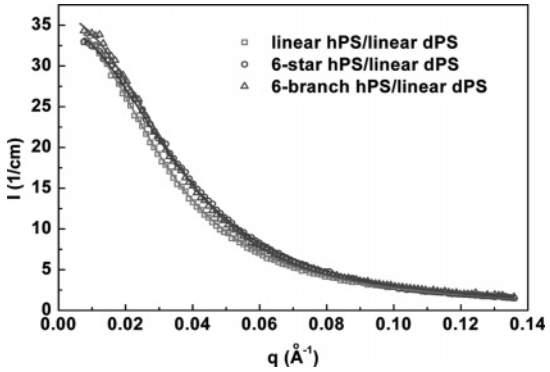

Figure 3. SANS experimental data with fits to the RPA for three different blends of 50 vol % hydrogenous PS (hPS) with linear deuterated PS of equal molecular weight at 120 °C.

correlation between segments in the outer arms of the branched polymer (A), $S_{AA}(q)$, can be obtained from the consideration of all the possibilities:

$$S_{AA}(q) = \frac{1}{f_A}S_{AA1} + \frac{f_A - f_B}{f_A f_B}S_{AA2} + \frac{f_B - 1}{f_B}S_{AA3} \quad (16)$$

$$S_{AA1}(q) = D(x_A), \qquad S_{AA2}(q) = F(x_A)^2,$$
$$S_{AA3}(q) = F(x_A)^2 E(x_{2B}) \quad (17)$$

$$E(x_{2B}) = e^{-x_{2B}}, \qquad x_{2B} = q^2 2n_B a^2/6 \quad (18)$$

where $x_A = q^2 n_A a^2/6$. The last correlation function $S_{AB}(q)$ captures the cross-correlation between segments of the outer branches of the polymer and the segments of the inner branches of the precursor and is given as

$$S_{AB}(q) = \frac{1}{f_B}S_{AB1}(q) + \frac{f_B - 1}{f_B}S_{AB2}(q) \quad (19)$$

$$S_{AB1}(q) = F(x_A)F(x_B), \qquad S_{AB2}(q) = F(x_A)F(x_B)E(x_B) \quad (20)$$

$$E(x_B) = e^{-x_B} \quad (21)$$

Finally, the form factor for an end-branched polymer can be obtained from eq 13 using eqs 14, 15, and 19. The structure factor for the 6-end pom-pom polymer was obtained similarly.

The parameters in the form factors such as n_i, N_i, and f_i are known values because the materials have been thoroughly characterized. By modeling the data using eqs 7 and 8 with the form factors appropriate for the polymers with various architectures, the values of χ_{eff} and a for the branched component (the value of a for the linear component was held fixed) can be determined for a polymer blend.

Examples of the scattering curves obtained at 120 °C for the linear *h*-PS/linear *d*-PS, 6-star *h*-PS/linear *d*-PS, and 6-branch/linear *d*-PS blends, each with 50 vol % *d*-PS component, are given in Figure 3. The scattering curves, while having very similar overall intensities, display clear differences. Over most of the observed q range, the scattering intensity is lowest for the blend of linear *h*-PS with linear *d*-PS. The intensity for the blend of 6-star *h*-PS with linear *d*-PS was the highest in the middle region of q (0.06−0.04 1/Å) but actually drops slightly below the intensity of the linear/linear blend at the smallest values of q. Therefore, even the shapes of the raw scattering curves evidence differences due to architectural variation. To account for change in molar volume with temperature, the value of 5.5 × 10^{-4} K^{-1} for the thermal expansion coefficient[36] was used. The only parameters allowed to vary to fit the raw data were the statistical segment length a and χ_{eff}. The values of the statistical segment lengths and χ_{eff} determined in this way are listed in Table 3. Strictly speaking, all the branched polymers have, in addition to non-styrenic chemistry at their cores, *sec*-butyl fragments at the ends of all the arms. Since the details of this chain end chemistry are identical for all branched polymers, we neglect these details in the extraction of the value of an effective χ. A second detail is the fact that some of the arms are "end-capped" with butadiene units for purposes of linking to the branch point. In a previous publication[37] we verified that the inclusion in the star chain of an average of 1.5 units of butadiene on the ends of the arms next to the core does not measurably perturb the value of χ_{eff} for a 4-arm star/linear blend. We will discuss below how these BD units might contribute to the effective interaction parameter for the branched molecules under study here.

Table 3. Statistical Segment Length and χ_{eff} Parameters for Isotopic Blends

	a (Å)[a]					$\chi_{eff} = A/T + B$	
polymer	120 °C	140 °C	160 °C	180 °C	200 °C	A (±0.1)	$B \times 10^4$ (±1.3)
linear	6.4	6.6	6.6	6.7	6.6	0.64	−13.5
6-star	6.4	6.6	6.4	6.5	6.5	0.82	−16.3
6-pom	5.7	5.8	5.9	5.9	5.9	0.93	−17.7
6-branch	5.7	5.8	5.8	5.8	5.8	0.93	−16.8
9-branch	5.8	5.8	5.9	5.9	5.9	0.99	−17.3
13-branch	5.8	5.9	6.0	5.9	5.9	1.17	−14.7

[a] Statistical segment length using segment volume = 100 cm^3/mol (±0.3 Å).

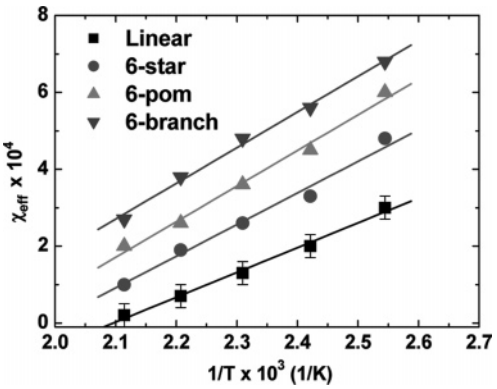

Figure 4. Variation in χ_{eff} for binary blends with chain ends constant, containing 50 vol % of the hPS component, linear or branched having 6 chain ends: (■) linear, (▲) 6-star with one branch point, (●) 6-pom with two branch points, and (▼) 6-branch with four branch points. Uncertainty bars for the linear/linear blends corresponding to ±0.3 × 10^{-4} are shown.

Effect of the Number of Branch Points. The variations of χ with temperature for blends of linear deuterated PS and branched PSs with different numbers of branch points from 1 to 4 and number of ends fixed at 6, as well as for the linear/linear isotopic blend, presented as a base case, are summarized in Figure 4. The uncertainties are presented for the linear/linear blend as an example. The interaction parameter for the isotopic linear/linear PS blend is positive and of the order of 10^{-4}. The precise magnitude (for example, 3.0 × 10^{-4} at 120 °C) was slightly higher than the value (2.2 × 10^{-4} at 120 °C) obtained by Bates and Wignall[38] for an isotopic linear/linear PS blend of the same composition (50 vol %) but much larger chain lengths (N = 1.15 × 10^4 for deuterated component and N = 8.7 × 10^3 for hydrogenous component).

None of the differences among the blends studied here can be ascribed to differences in the overall chain sizes of the components, as they are as nearly the same as reasonably achievable by synthesis. An estimate using the Gaussian field theory for the effect of overall chain molecular weight also supports this statement. Thus, the larger magnitude of χ_{eff} for the blend of 6-star as compared to the magnitude of χ_{eff} for the isotopic linear/linear blend, for instance, must be due to an architecture effect (including branch points). The magnitude of the increase ($\sim 1.2 \times 10^{-4}$) due to the introduction of 1 branch point with 6 arms in one component agrees quantitatively with Greenberg et al.'s result.[18] The value of χ_{eff} for the blend with the 6-pom polymer having two branch points was larger than that for the 6-star/linear blend. Since the precursor polymer for the 6-pom polymer actually contains a two arm junction consisting of the difunctional initiator having two *sec*-butyl fragments, the 6-pom polymer can alternatively (at a higher level of detail) be considered as having three junction points. In any case, when the number of junction points is increased in going from the 6-star to the 6-pom branched component, the value of χ_{eff} also increases. When the branched component was changed from the 6-pom with 2 or 3 junction points to the 6-branch chain with 4 junction points, the value of the effective interaction parameter increased further. So we saw consistently that the magnitude of the effective interaction parameter increased as the number of junction points in the branched component increased from 0 (linear) to 1 (6-star) to 2 or 3 (6-pom) to 4 (6-branch).

The slopes of all the lines in Figure 4 and the statistical segment lengths determined from the fitting of the SANS data are listed in Table 3. The slopes for the three branched PS/linear blends were similar and differed from that for the linear/linear blend. The difference in slope between the linear/linear blend and branched PS/linear blends could conceivably be caused by both the different core structure and the larger number of chain ends of the branched polymers. There might be a small difference between the blends with linear polymer and those with the branched polymers in the temperature-dependent portion of χ_{eff}, but the magnitude of this temperature-dependent contribution varied little among the blends with the different branched polymers with 6 ends. If the difference in slope between the 6-star blend and the other two blends with branched chains is significant, it is due to the different core structures in the various molecules.

Effect of Number of Chain Ends. SANS measurements of binary blends of linear deuterated PS and three molecules in which the number of branch points was fixed at 4 and the number of chain ends varied among 6, 9, and 13 elucidated the effect of the number of chain ends on χ_{eff}. The variations in χ_{eff} with temperature for the three blends are plotted in Figure 5 along with data for the linear/linear blend. The slopes of all the curves in Figure 5 and the corresponding statistical segment lengths from the fitting of the SANS data are listed in Table 3. From the analysis of blends with star polymers above, we would anticipate the general trend of χ_{eff} increasing with increasing functionality of branch points and shortening of branches. Indeed, as the hydrogenous polymer changed from 6-branch to 9-branch to 13-branch, the value of χ_{eff} increased.

Over the temperature range investigated most of the change appears as simply a parallel shift up as the number of chain ends is increased, suggesting that much of the change is entropic. However, closer analysis reveals that the slopes of the fitted lines also increase somewhat as the number of chain ends increases. While the increase in slope going from 6-branch to 9-branch blends is within the experimental uncertainty, both the enthalpic and entropic contributions for the 13-branch blend are significantly higher than those for the other two blends in this group.

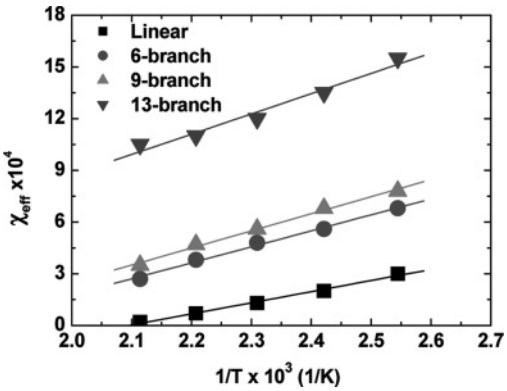

Figure 5. Variation in χ_{eff} for binary blends containing 50 vol % of the linear hPS component or branched component having 4 branch points: (■) linear, (●) 6-branch, (▲) 9-branch, and (▼) 13-branch. The uncertainties are of the order of the size of the plotting symbols.

In addition to pure architectural effects, the changes in χ_{eff} may thus have contributions due to changes in the number of specific end groups. It is also true that the linking agents used to make the different end-branched stars differed in their detailed structure. In particular, the 13-end branch chain includes outer junction points containing two silicon atoms rather than one. However, we believe it is likely that the more obvious change in molecule chemistry arising from moving from 6 to 9 to 13 ends with butyl fragments contributes more strongly to the change in χ_{eff} than does the more subtle change in junction chemistry. Indeed, a plot of the enthalpic contribution to χ_{eff} (parameter A in Table 3), subtracting out the value for the isotopic linear/linear blend, is roughly linear in the number of butyl fragments, as we discuss below. We note that these group specific contributions should become increasingly minor as the lengths of the branches increase. Nonetheless for very long chains, if the group specific contributions scale as N^{-1}, they will dominate the entropic contributions due to architecture which are expected to scale as $N^{-3/2}$ (see eq 5).

How close did the branch/linear blends come to bulk separation? As an imprecise estimate, we consider a comparison with the critical value of χ_{eff} (χ_c) for an isotopic, compositionally symmetric linear/linear blend. A mean-field estimation for χ_c in the Flory approach is $\chi_c = 2/N_c$. Specifically, χ_c for a symmetric linear/linear blend analogue to the 13-branch/linear blend, in which $N_{branch} = 322$, is ca. 6×10^{-3}. Even the 13-branch/linear blend was still far from bulk phase separation at the lowest temperature considered. While the more highly branched chains are less miscible with linear analogues, the branching could be still higher or the molecular weight about a factor of 4 higher before bulk separation would be expected to be a problem. This suggests such blends could be much more useful than blends of linear chains and dendrimers, which readily phase separate.

Comparison with Theory. Since the structure factors are known, χ_ϵ can be calculated using eqs 3 and 4 once the segment length is fixed. The statistical segment length fit for the linear/linear isotopic blend was in good agreement with the reference value, $a = 6.7$ Å.[39] The values of statistical segment length for the star are the same as those for the linear chains within the uncertainties, while the statistical segment lengths fit for the other branched polymers were smaller. This is perhaps surprising from the point of view that the star should be stretched relative

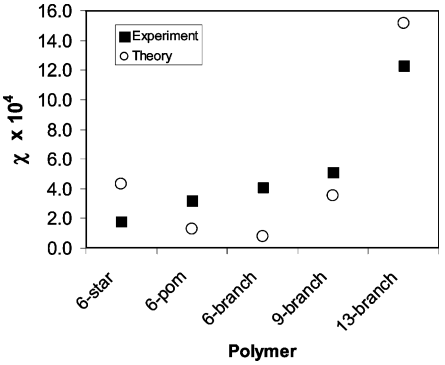

Figure 6. Comparison of χ_ϵ values (open circles) for blends of linear and branched chains calculated from the Gaussian field theory assuming $a = 6.2$ Å with the χ_ϵ values (filled squares) determined by fitting the experimental data at 120 °C, allowing a to vary as a fitting parameter as described in Table 3 and then subtracting the contribution due to isotopic labeling from the overall value of χ_{eff}.

to the linear polymer, and the 13-branch has outer branch points which are nearly as high in functionality as the star.

Although it may appear that one could use these different values of a directly in the structure factors, resulting in an apparent conformational asymmetry contribution to χ, it is perhaps more sensible to use an average value of a. One reason for differences in a is to account for stretching or compression of branches in the branched chain. This stretching likely does not occur uniformly throughout the chain; for instance, we expect the chain near high-functional branch points to be more strongly stretched than is that part of the chain farther from the joint. Since the monomers on the linear and branched chains are identical, it is perhaps reasonable to assume that the local density correlations on the monomer scale are very similar for monomers from either component. This would suggest again that the mismatches in the single-chain structure factor are primarily on length scales greater than the monomer size. This conclusion seems to be borne out below by the trends in the end-branched series and the good agreement in the overall magnitude of χ_{eff} with that predicted from our theory that does not have conformational asymmetry. (Conformational asymmetry contributions are much larger.) Thus, for the purposes of comparison, an average segment length of 6.2 Å was used in the theory for all the polymers, although the experimentally derived values of a are somewhat smaller for the branched chains. The values of all other molecular parameters were taken to be those from the experimental determination of χ_{eff}.

The theoretically estimated χ values for the blends with branched components of different architectures are compared in Figure 6 with χ_ϵ values obtained from fitting the experimental SANS data at 120 °C and subtracting away an estimate of the contribution due to isotopic labeling. The general increase in the theoretical value with an increase in the number of chain ends for the chains with a fixed number of branch points matches the general trend in the experimental values, although the magnitudes differ. However, the trend seen for the variation with increasing number of branch points with fixed number of ends was the reverse of that seen in the experimental values.

We speculate that this is because the theoretical calculation did not capture enthalpic contributions to χ_{eff} due to differences in the chemistries of the various junction points. For all chains but the linear chains, all chain ends are *sec*-butyl fragments. For the 6-star polymer the arms are connected at one junction point with a silane-type structure. The outside branching points for a 6-pom, a 6-branch, a 9-branch, and a 13-branch chain also have structures dictated by the type of linking agent used.

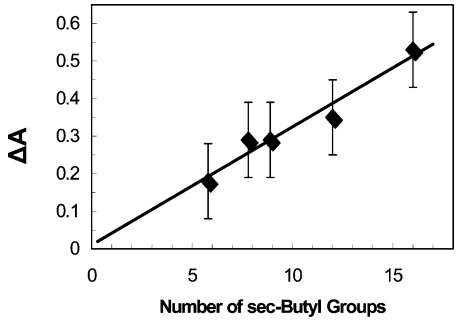

Figure 7. Increase ΔA over the value for the linear dPS/linear hPS blend of the A parameter determining the temperature dependence of χ_{eff} (see Table 3) vs the number of *sec*-butyl groups in the branched polymer molecule. The line is a linear fit to the data.

However, the precursor chain of the 6-pom is connected in the middle by a difunctional initiator having two *sec*-butyl fragments, and the precursor chains of the 6-branch, 9-branch, and 13-branch all have a core composed of the trifunctional initiator having three *sec*-butyl fragments. Thus, if the *sec*-butyl fragments on the chain ends result in enthalpic effects for the bulk thermodynamics, the *sec*-butyl fragments on the junctions will as well. Figure 7 plots the change over the linear/linear blend of the A parameter describing the temperature dependence of χ_{eff} vs the number of *sec*-butyl fragments in the branched polymer molecule. While various factors, such as the number and type of other branching groups, need to be accounted for, the linear trend in Figure 7 is consistent with the possibility that one can associate an enthalpic contribution to χ_{eff} for each *sec*-butyl fragment. We note that in the limit of very long arms and linear chains the entropic contribution predicted by the theory scales as $N^{-3/2}$, which is expected to be subdominant to the $O(N^{-1})$ enthalpic contribution from specific branch or end groups. Nonetheless, the entropic contribution from architecture may still be comparable in significance for moderately long chains.

A related issue is the role of packing on the mixing free energy. For long enough branched and linear chains, differences in packing are expected to occur primarily at the junction and end groups. Indeed, the measured densities in the glassy state of the different molecules studied here are indistinguishable, and so we do not expect compressibility effects to be significant. The packing differences near individual junction or end groups, however, can be expected to be absorbed into group specific contributions to χ_{eff} together with the enthalpic contributions mentioned above. While the temperature dependence shown in Figure 7 suggests that the contributions are predominantly enthalpic, further systematic studies, for instance by varying chain lengths and branching groups, will be necessary to check these issues.

It is also of interest to see how well the theory predicts changes in the size of the chains *in solution* with changes in architecture. Again, only a crude comparison is possible at the present, but this comparison suggests good qualitative agreement between theory and experimental results. The value of the radius of gyration is readily extracted from the theory by simply analyzing the structure factor $S(q)$. For sufficiently small values of q the structure factor is well approximated by the equation

$$S(q) \approx 1 - \frac{q^2 R_g^{\,2}}{3} + \ldots \qquad (22)$$

The radii of gyration extracted from the structure factors with a taken to be 6.2 Å are shown in Figure 8. These R_g values

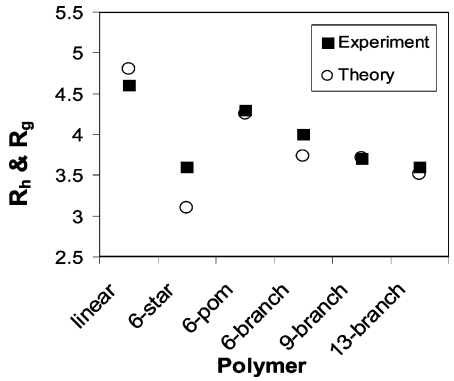

Figure 8. Comparison between the radii of gyration (open circles) of the various branched polymers calculated from the Gaussian field theory and the hydrodynamic radii (see Table 2) (filled squares) measured by dynamic light scattering in good solvent (toluene, 25 °C).

Table 4. Interaction Parameter Values at 220 °C for PS Isotopic Blends Discussed in Ref 18

blend	χ at 220 °C ($\times 10^{-5}$)	$\Delta\chi$ ($\times 10^{-5}$)[b]	theory χ from universal expression ($\times 10^{-5}$)
linear/linear	6	0	
4-arm star/linear	9[a]	3	2.2
5-arm star/linear	9[a]	3	4.3
6-arm star/linear	13[a]	7	7.6
hydrogenous 8-arm star/linear	17	11	7.4
hydrogenous 12-arm star/linear	35	29	152
hydrogenous 14-arm star/linear	36	30	87
deuterated 15-arm star/linear	71	65	214
deuterated 16-arm star/linear	71	65	266
hydrogenous 17-arm star/linear	37	31	315
hydrogenous 21-arm star/linear	42	36	100

[a] Averages of χ between labeling schemes. [b] Difference between the experimental value of χ for a given blend and the value measured for the linear/linear isotopic blend.

should be characteristic of the behavior of chains in a theta solvent. Making measurements at exactly the theta state for each of these different architectures is not a simple matter, as the theta temperature in a given solvent varies with the architecture of the chain. Thus, we have chosen to make a qualitative comparison with the hydrodynamic radii of gyration measured in good solvent, presented earlier in Table 2. Of course, the "goodness" of solvent at a fixed temperature is also a function of the architecture, so the values of hydrodynamic radius have not been measured in rigorously identical solvent conditions, but we anticipate that for rather good solvent (far from the theta state) these differences in solvent quality with architecture will not be very important. If the statistical segment lengths were properly matched, the hydrodynamic radius would be expected to be $0.667R_g$ in the theta state but could be comparable to or larger than R_g in a good solvent. In fact, as shown in Figure 8, the experimental values of R_h in good solvent and theoretical values of theta state R_g are quite similar, and certainly the theory captures the main trends observed experimentally. These trends are (1) that the star has the smallest chain size in solution and (2) that otherwise the chain size decreases monotonically with "increased branching" as linear > 6-pom > 6-branch > 9-branch > 13-branch.

Conclusion

The effects of the number of branch points and number of chain ends in a branched chain on bulk thermodynamics in binary blends of well-defined, regularly branched polystyrenes with their linear analogues were examined using SANS.

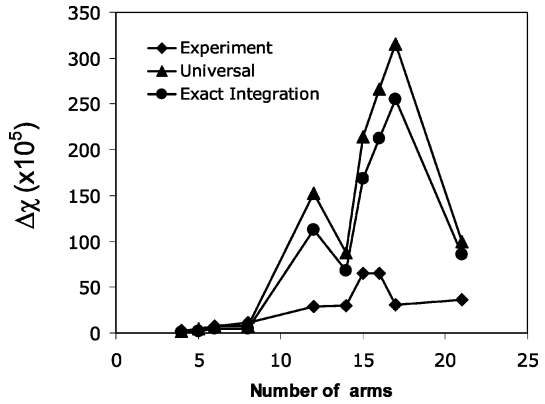

Figure 9. Plot of the variation in χ corrected for isotopic effects as a function of the number of arms in the star in various star/linear isotopic blends reported by Greenberg et al.[18] experimental (diamonds), universal theoretical approximation (triangles), and exact theoretical calculation (circles).

The structure factors for the end-branched polymers were developed using the expression of Benoit. The magnitude of the effective interaction parameter increased as the number of branch points increased while the number of chain ends was fixed. The value of the effective interaction parameter also increased with increasing number of chain ends. A Gaussian field theory is successful in predicting the important qualitative variations in the size of the branched molecules in solution with topology. This theory also reasonably predicts the overall magnitude and trend in bulk χ_{eff} with the number of chain ends for constant number of branch points but does not succeed in capturing the changes in χ_{eff} with changes in the number of branch points for constant number of chain ends. This may be due to the fact that the theory neglects differences in the chemistries of the branch points. Although such effects diminish as the branches become sufficiently long, they may still dominate the entropic effects due to architecture, which are predicted to vanish even more quickly.

Acknowledgment is made to the donors of the American Chemical Society Petroleum Research Fund for partial support of this research. The authors are also grateful for partial support from an Ohio Board of Regents challenge grant. Neutron scattering experiments were performed at the NIST facilities supported by the NSF under Agreement DMR-9986442. M.D.F. and J.L. thank Dr. Derek Ho for assistance with the SANS measurements and Dr. Boualem Hammouda for assistance with developing the structure factors.

Appendix

In ref 18, incorrect values for χ calculated from the theory of Fredrickson et al.[21] were reported for the blends containing stars with more than 10 arms. In Table 4 we report the correct values in a format consistent with that of Table III in ref 18. The quantity $\Delta\chi$ used in ref 18 and in this appendix is the experimental value of χ attributed to architectural effects alone (i.e., χ_ϵ), obtained by subtracting the experimentally measured value of χ for a linear/linear isotopic blend from that for a given blend of branched and linear chains. We note that all these blends were of off-symmetric composition (~18 wt % in branched chain). When the correct theoretical values are considered, the agreement between theory and experiment is not as close as incorrectly reported in ref 18.

In Figure 9 we plot the experimental values of χ corrected for the isotopic contribution with values from the theoretical calculation using the universal expression and also the theoretical

values computed using the exact expression. For the lowest numbers of arms there is quantitative agreement between the experiment and universal approximate expression. For numbers of arms above 10 the theoretical values exhibit the same qualitative trends seen in the experimental data, but the effects are predicted to be much larger than seen experimentally. Using the exact theoretical expression improves the agreement slightly for numbers of arms greater than 10, reducing the theoretical values by about 15%. However, the agreement between theory and experiment is less good with the exact calculation for blends with stars having fewer than 10 arms.

References and Notes

(1) Kharchenko, S. B.; Kannan, R. M.; Cernohous, J. J.; Venkataramani, S. *Macromolecules* **2003**, *36*, 399.
(2) Roberston, C. G.; Roland, C. M.; Puskas, J. E. *J. Rheol.* **2002**, *46*, 307.
(3) Suneel, D. M. A.; Buzza, D. J.; Groves, D. J.; McLeish, T. C. B.; Parker, D.; Keeney, A. J.; Feast, W. J. *Macromolecules* **2002**, *35*, 9605.
(4) Hay, G.; Mackay, M. E.; Hawker, C. J. *J. Polym. Sci., Part B: Polym. Phys.* **2001**, *39*, 1766.
(5) Mackay, M. E.; Carmenzini, G.; Sauer, B. B.; Kampert, W. *Langmuir* **2001**, *17*, 1708.
(6) Groves, D. J.; McLeish, T. C. B.; Ward, N. J.; Johnson, A. F. *Polymer* **1998**, *39*, 3877.
(7) Bates, F. S.; Muthukumar, M.; Wignall, G. D.; Fetters, L. J. *J. Chem. Phys.* **1988**, *89*, 535.
(8) Sakurai, S.; Hasegawa, H.; Hashimoto, T.; Hargis, I. G.; Aggarwal, S. L.; Han, C. C. *Macromolecules* **1990**, *23*, 451.
(9) Sakurai, S.; Jinnai, H.; Hasegawa, H.; Hashimoto, T.; Han, C. C. *Macromolecules* **1991**, *24*, 4389.
(10) Beaucage, G.; Stein, R. S.; Hashimoto, T.; Hasegawa, H. *Macromolecules* **1991**, *24*, 3443.
(11) Jones, T. D.; Chaffin, K. A.; Bates, F. S.; Annis, B. K.; Hagaman, E. W.; Kim, M. H.; Wignall, G. D.; Fan, W.; Waymouth, R. *Macromolecules* **2002**, *35*, 5061.
(12) Bates, F. S.; Wignall, G. D.; Koehler, W. C. *Phys. Rev. Lett.* **1985**, *55*, 2425.
(13) Bates, F. S.; Dierker, S. B.; Wignall, G. D. *Macromolecules* **1986**, *19*, 1938.
(14) Faust, A. B.; Sremcich, P. S.; Gilmer, J. W.; Mays, J. W. *Macromolecules* **1989**, *22*, 1250.
(15) Russell, T. P.; Fetters, L. J.; Clark, J. C.; Bauer, B. J.; Han, C. C. *Macromolecules* **1990**, *23*, 654.
(16) Chen, Y. Y.; Lodge, T. P.; Bates, F. S. *J. Polym. Sci., Part B: Polym. Phys.* **2000**, *38*, 2965.
(17) Chen, Y. Y.; Lodge, T. P.; Bates, F. S. *J. Polym. Sci., Part B: Polym. Phys.* **2002**, *40*, 466.
(18) Greenberg, C. C.; Foster, M. D.; Turner, C. M.; Corona-Galvan, S.; Cloutet, E.; Quirk, R. P.; Bulter, P. D.; Hawker, C. *J. Polym. Sci., Part B: Polym. Phys.* **2001**, *39*, 2549.
(19) Greenberg, C. C.; Foster, M. D.; Turner, C. M.; Corona-Galvan, S.; Cloutet, E.; Bulter, P. D.; Hammouda, B.; Quirk, R. P. *Polymer* **1999**, *40*, 4713.
(20) Greenberg, C. C. Ph.D. Dissertation, The University of Akron, Akron, 1999.
(21) Fredrickson, G. H.; Liu, A. J.; Bates, F. S. *Macromolecules* **1994**, *27*, 2503.
(22) Martter, T. D.; Foster, M. D.; Yoo, T.; Xu, S.; Lizzaraga, G.; Quirk, R. P.; Butler, P. D. *Macromolecules* **2002**, *35*, 9763.
(23) Martter, T. D.; Foster, M. D.; Ohno, K.; Haddleton, D. M. *J. Polym. Sci., Part B: Polym. Phys.* **2002**, *40*, 1704.
(24) Hutchings, L. R.; Richards, R. W. *Macromolecules* **1999**, *32*, 880.
(25) Lee, J. S.; Quirk, R. P.; Foster, M. D. *Macromolecules* **2005**, *38*, 5381.
(26) Grayce, C. J.; Schweizer, K. S. *Macromolecules* **1995**, *28*, 7461.
(27) Patil, R.; Schweizer, K. S.; Chang, T. *Macromolecules* **2003**, *36*, 2544.
(28) Singh, C.; Schweizer, K. S. *Macromolecules* **1997**, *30*, 1490.
(29) Schweizer, K. S. *Macromolecules* **1993**, *26*, 6050.
(30) Patil, R.; Schweizer, K. S.; Chang, T. M. *Bull. Am. Phys. Soc.* **2002**, *47*, 839.
(31) Lee, J. S.; Quirk, R. P.; Foster, M. D.; Wollyung, K. M.; Wesdemiotis, C. *Macromolecules* **2004**, *37*, 6385.
(32) Zimm, B. H.; Stockmayer, W. H. *J. Chem. Phys.* **1949**, *17*, 1301.
(33) deGennes, P. G. *Scaling Concepts in Polymer Physics*; Cornell University Press: Ithaca, NY, 1979.
(34) Benoit, H. *J. Polym. Sci.* **1953**, *17*, 507.
(35) Hammouda, B. *Adv. Polym. Sci.* **1993**, *106*, 87.
(36) Brandrup, J.; Immergut, E. H. *Polymer Handbook*, 3rd ed.; John Wiley & Sons: New York, 1989.
(37) Lee, J. S.; Quirk, R. P.; Foster, M. D. *Macromolecules* **2004**, *37*, 10199.
(38) Bates, F. S.; Wignall, G. D. *Phys. Rev. Lett.* **1986**, *57*, 1429.
(39) Wignall, G. D.; Ballard, D. G. H.; Schelten, J. *Eur. Polym. J.* **1974**, *10*, 861.

MA060023J